Aalborg Universitet

Higher Derivatives Newton-Based Extremum Seeking for Constrained Inputs

Karimi, Farzaneh; Ramezani, Hossein; Izadi-Zamanabadi, Roozbeh; Mojiri, Mohsen

Higher Derivatives Newton-based Extremum Seeking for Constrained Inputs

Farzaneh Karimi
Dept. of Elec. and Comp. Eng.
Isfahan Univ. of Tech.
Isfahan, 84156-83111, Iran
farzaneh.karimi@iut.ac.ir

Hossein Ramezani
Dept. of Mech. and Elec. Eng.
Univ. of Southern Denmark
Sønderborg, Denmark
ramezani@sdu.dk

Roozbeh Izadi-Zamanabadi
Dept. of Elec. Sys.
Aalborg University
Aalborg, Denmark
riz@es.aau.dk

Mohsen Mojiri
Dept. of Elec. and Comp. Eng.
Isfahan Univ. of Tech.
Isfahan, 84156-83111, Iran
mohsen.mojiri@iut.ac.ir

Abstract—**This paper introduces a fast learning mechanism to address constrained input in the higher derivatives Newton-based extremum seeking. The proposed algorithm has a two-time-scale structure consisting of: a compensation mechanism (i.e. an anti-windup compensator) with fast dynamics that compensates for the effect of the constrained input, and a slow subsystem to maximize the map's higher derivatives by regulating the output. The practical asymptotic stability of the new ES algorithm is proved using a modified version of the singular perturbation method. The effectiveness of the proposed algorithm is demonstrated using simulations.**

I. Introduction

Extremum Seeking (ES) is a real-time and model-free optimization tool that determines the extremum value of an unknown map which is known to have an extremum. Leblanc published the first known ES algorithm in [1] and the initial ES approach is gradient-based which uses sinusoidal signals, as perturbation signals, to estimate the gradient of the map. The first stability analysis for an ES system was presented by Wang and Krstic [2]. The stability analysis which was based on classical singular perturbation and averaging methods sparked revived interest in the field. Since 2000 the ES method has seen important theoretical progressions [3]. Some other worthy extensions of ES are fixed-time ES [4], normalized ES [5] and stochastic ES [6].

Newton-based ES was extensively discussed in [7]. This approach employs an estimate of the map Hessian inverse and makes the algorithm user-assignable as the convergence does not depend on the second derivative anymore. In [8], a generalization of the Newton-based ES is presented to maximize a higher derivative of the map. By appropriately demodulating the map output, the ES algorithm maximizes the nth derivative asymptotically only via map measurements.

Regarding the practical application of ES algorithm, [9] describes a refrigeration system where the desired operating point is located at the maximum slope. This work has been the motivation of many researches including [8]. As the effect of delay in practical systems is important, in [10] a Newton-based ES extension scheme is designed for higher derivatives of unknown dynamic maps under delays.

Another important phenomena which is the main focus of current study and that can cause problems in ES algorithm is windup. This phenomena is due to the saturation of actuator which can occur in control applications. Handling the constrained input in gradient-based ES algorithms is not new as [11], [12] and [13] have studied, dead zone, saturation

and mixed-integer, respectively. However, to the best of our knowledge, no paper has addressed the problem of higher derivatives Newton-based ES in the presence of constraints. In this paper the work of [8] on the Newton-based ES method for maximizing higher derivative is extended to handle the saturated input case. The saturated input is modeled by a function as follows:

$$D_{sat}(u, \boldsymbol{u_s}) = \begin{cases} u_{max} & u \geq u_{max} \\ u & u_{min} < u < u_{max} \\ u_{min} & u \leq u_{min} \end{cases} \quad (1)$$

where $\boldsymbol{u_s} = [u_{min}, u_{max}]$ and is known.

In the proposed scheme, there are two main components. The first one is a higher derivatives Newton-based ES that can maximize the map's higher derivatives by regulating the output. The second component which is the contribution of this paper is a fast learning mechanism in the form of an anti-windup compensator that can compensate for the effect of saturated input. Separating these two components can be done using a temporal separation, where the ES and the learning mechanism can be modeled as slow and fast subsystems, respectively. The stability analysis of the proposed scheme will be provided in details using the singular perturbation techniques.

The paper is formed as follows: The problem formulation and the proposed approach are given in Section II. The stability properties are discussed in three steps in Section III. Section IV demonstrates the effectiveness of the proposed approach using a simulation example.

A. Notation and Definitions

Definition 1. *[14], A continuous, bounded function $g(t, x)$: $[0, \infty) \times D \to \mathbb{R}^n$ is said to have a well-defined average g_{av} if the limit*

$$g_{av}(x) = \lim_{T \to \infty} \frac{1}{T} \int_t^{t+T} g(\tau, x) d\tau \quad (2)$$

exists and $\forall (t, x) \in [0, \infty) \times D_0$

$$\left\| \frac{1}{T} \int_t^{t+T} g(\tau, x) - g_{av}(x) d\tau \right\| \leq k\sigma(T), \quad (3)$$

for every compact set $D_0 \subset D$, where k is a positive constant (possibly dependent on D_0) and $\sigma : [0, \infty) \to [0, \infty)$ is a strictly decreasing, continuous, bounded function such

that $\sigma(T) \to 0$ as $T \to \infty$. The function σ is called the convergence function.

Definition 2. *[15], The system $\dot{x} = f(x,u)$, $x \in R^n, u \in R^m$, and the locally Lipschitz map $f : R^n \times R^m \to R^n$ is said to be input-to-state practically stable (ISPS) if there exists a function $\mathbf{l}$ of class $\mathcal{KL}$, a function $\mathbf{p}$ of class $\mathcal{K}$ and a non-negative constant d such that, for each initial condition $x(0)$ and each measurable essentially bounded control $u(.)$ defined on $[0, \infty)$, the solution $x(.)$ of the system (1) exists on $[0, \infty)$ and satisfies:*

$$|x(t)| \leq \mathbf{l}(x(0), t) + \mathbf{p}(\|u\|) + d \qquad \forall t \geq 0 \qquad (4)$$

II. PROBLEM FORMULATION

To show the main idea of this paper, we first consider the following static single-input-single-output (SISO) plant with input saturation:

$$y = h(D_{sat}(u, \boldsymbol{u_s})) \qquad (5)$$

To simplify, denote $D_{sat}(u, \boldsymbol{u_s})$ as $D(u)$. The two initial assumptions on $h(D(u)) : \mathbb{R} \to \mathbb{R}$ are listed below:

Assumption 1. *Consider the smooth function $h(u) : \mathbb{R} \to \mathbb{R}$ and the set*

$$u^* = \{u \in \boldsymbol{u_s} | h^{(n+1)}(u) = 0 \ h^{(n+2)}(u) < 0\} \qquad (6)$$

to be a collection of maximums where $h^{(n)}(.)$ is locally concave.

Assumption 2. *The system (5) is well-defined average, according to the definition 1.*

In essence, the goal is to maximize the nth derivative of the system in the presence of a constrained input. On the other hand:

$$\max_{u \in R} h^{(n)}(D(u)) := \max_{u \in \boldsymbol{u_s}} h^{(n)}(u) \qquad (7)$$

where only the output signal $y = h(D(u))$ is measurable.

The existence of an integrator at the ES algorithm in presence of the saturated actuator causes unfavorable behavior, which is similar to the "wind up" phenomenon in the classical control, i.e. the calculated control variable exceeds the operational limits of the physical actuator. As a result, the actual input differs from the presumed input. Due to this mismatch, the integrator will keep accumulating the error hence makes the recovering of input signal to be time consuming.

As explained in [12], by using a penalty function method, the constrained optimization ES problem can be tackled. In general, a penalty function $Q_b(u, \boldsymbol{u_s})$ serves as a measure of a violation of the constraints. The measure of violation is nonzero when the constraints are violated and is zero when otherwise. If $Q_b(u, \boldsymbol{u_s})$ is selected properly, $\frac{\partial Q_b}{\partial u}$ can be used to guide the input signal out of the saturation zone. To do this, any penalty function should satisfy the following equation:

$$\begin{cases} \frac{\partial Q_b}{\partial u}(u, \boldsymbol{u_s}) < 0 & u \geq u_{max} \\ \frac{\partial Q_b}{\partial u}(u, \boldsymbol{u_s}) = 0 & u_{min} < u < u_{max} \\ \frac{\partial Q_b}{\partial u}(u, \boldsymbol{u_s}) > 0 & u \leq u_{min} \end{cases} \qquad (8)$$
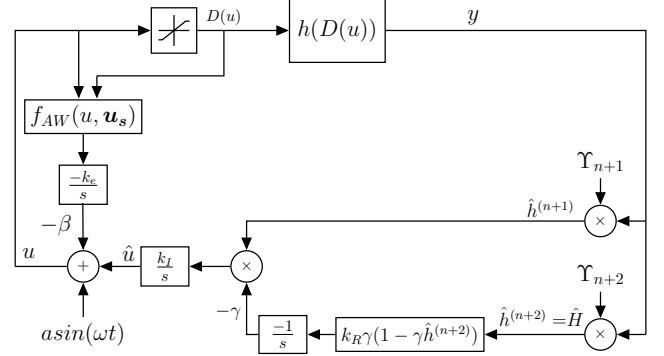

Fig. 1: Higher derivatives Newton-based ES saturated input.

Some of the functions that can be selected are listed below:
1) The logarithmic penalty function:

$$Q_b^{log}(.) = -ln((u - D(u))^2 + \varepsilon), \ \varepsilon > 0 \qquad (9)$$

2) The inverse penalty function:

$$Q_b^{inv}(.) = \frac{1}{(u - D(u))^2 + \varepsilon}, \ \varepsilon > 0 \qquad (10)$$

3) The polynomial penalty function:

$$Q_b^p(.) = -(u - D(u))^m \qquad m = 2n \qquad n = 1, 2, .. \qquad (11)$$

For classical ES, [12] through simulations indicates that an anti-windup compensator using a penalty function can ensure that the input returns to and remains in the desired domain. Inspired by this idea, the following anti-windup function is defined:

$$f_{AW}(u, \boldsymbol{u_s}) = \frac{\partial Q_b}{\partial u}(u, \boldsymbol{u_s}) \qquad (12)$$

The proposed structure of the Newton-based anti-windup ES for maximization of higher derivatives is illustrated in Fig 1. The governing closed-loop equations of Fig 1 are

$$\dot{\beta} = -k_e f_{AW}(u, \boldsymbol{u_s}) \qquad (13a)$$

$$\dot{\hat{u}} = -k_I \gamma \Upsilon_{n+1} h(D(u)) \qquad (13b)$$

$$\dot{\gamma} = k_R \gamma \left(1 - \gamma \Upsilon_{n+2} h(D(u))\right) \qquad (13c)$$

where $u = -\beta + \hat{u} + a \sin(\omega t)$ and the demodulation signal Υ_j and the normalizing gain C_j are given as follows:

$$\Upsilon_j(t) = C_j \sin\left(j\omega t + \frac{\pi}{4}(1 + (-1)^j)\right) \qquad (14a)$$

$$C_j = \frac{2^j j!}{a^j}(-1)^{\left(\frac{j - |\sin(\frac{j\pi}{2})|}{2}\right)} \qquad (14b)$$

The demodulated signals $\hat{h}^{(j)} = y\Upsilon_j$ are meant to, on average, estimate the gradient $(h^{(j+1)})$ and the Hessian $(h^{(j+2)})$ of the jth derivative of the map [8]. As mentioned in [16], there are two essential parts to Newton-based ES algorithm: 1- Estimate of the Hessian of $\hat{h}^{(n)}(.)$, denoted as $\hat{H}$, using $\Upsilon_{n+1}(t)$.

2- Estimate the inverse of the generated Hessian $\left(\gamma \approx \hat{H}^{-1}\right)$ using a differential Riccati equation given in (13c).

To avoid exceeding input's limitations and thereby removing the the anti-windup effect on the system's steady-state, following assumption is proposed:

Assumption 3. *There exists $\alpha^* > 0$ such that for any $\alpha \in (0, \alpha^*]$ the following inequality holds*

$$\min\{\inf\{|u_{max} - (u^* + a\sin(\omega t))|\},$$
$$\inf\{|u_{min} - (u^* + a\sin(\omega t))|\} \geq \alpha \quad (15)$$

III. STABILITY

The stability analysis utilizes a two time-scale decomposition of the system's dynamics (13). The system has three integrators where one of them is going to have a faster convergence than the other two. Considering a high integrator gain k_e, the anti-windup integrator would be the fast dynamics one. Therefore, the other two integrator gains can be redefined as follows:

$$k_I = \omega\epsilon\hat{k}_I = O(\omega\epsilon) \quad (16a)$$
$$k_R = \omega\epsilon\hat{k}_R = O(\omega\epsilon) \quad (16b)$$

where $\hat{k}_I, \hat{k}_R > 0$ and ϵ is a small positive constant. Now, by defining a time-scale transformation as $\tau = \omega t$, we have:

$$\omega\frac{d\beta}{d\tau} = -k_e f_{AW}(u, \boldsymbol{u_s}) \quad (17a)$$
$$\frac{d\hat{u}}{d\tau} = -\epsilon\hat{k}_I\gamma\hat{\Upsilon}_{n+1}h(D(u)) \quad (17b)$$
$$\frac{d\gamma}{d\tau} = \epsilon\hat{k}_R\gamma\left(1 - \gamma\hat{\Upsilon}_{n+2}h(D(u))\right) \quad (17c)$$

where $\hat{\Upsilon}_j = C_j \sin\left(j\tau + \frac{\pi}{4}(1 + (-1)^j)\right)$.

The two-time scale structure of (17) is in a singular perturbation model ([14]) with ϵ being the perturbation parameter. In this equation the small value of ϵ shows the slower dynamic of (17b) and (17c) compared to (17a). Hereafter we call the fast dynamic of (17a) as the boundary layer model and the slow dynamics of (17b) and (17c) as the reduced system model (since the overall model reduces to the slow dynamics after the fast part is converged).

To investigate the stability of the overall system, according to [14] the stability of each subsystem can be studied separately. Replacing β in (17a) with β^{bl}, the boundary layer subsystem is as follows:

$$\omega\frac{d\beta^{bl}}{d\tau} = -k_e f_{AW}(u, \boldsymbol{u_s}) \quad (18)$$

The following lemma can be used for the stability proof of (18).

Lemma 1. *Let the assumption 3 be satisfied then for $t \in [t_0, t_l]$, the boundary layer subsystem is ISPS.*

Proof. Following cases are considered:

Case 1: $u(t_0) \in \boldsymbol{u_s}$:
According to the property of the penalty function given in (8), $f_{AW}(u, \boldsymbol{u_s}) = 0$, hence

$$\frac{d\beta^{bl}}{d\tau} = 0 \quad (19)$$

so $\beta^{bl}(t) = \beta^{bl}(t_0)$.

Case 2: $u(t_0) \notin \boldsymbol{u_s}$:
Among the possible penalty functions, the proof of *Case 2* is given for $Q_b^p(.) = -(u - D(u))^m$. It will be later shown that the proof for other penalty functions can be resulted from the given proof. Substituting (11) for $m = 2$ into (12) and then into (18) we have:

$$\frac{d\beta^{bl}}{d\tau} = k_e u(\tau) - k_e D(u) = k_e u(\tau) - k_e \overline{u}_s \quad (20)$$

where $\overline{u}_s \in \{u_{min}, u_{max}\}$. Therefore from (**??**)

$$\frac{d\beta^{bl}}{d\tau} = k_e(\hat{u} + a\sin(\tau) - \beta^{bl}(\tau)) - k_e\overline{u}_s \quad (21)$$

and by defining $\hat{b} = \hat{u} + a\sin(\tau)$, the dynamics of the boundary layer subsystem is simplified as follows:

$$\frac{d\beta^{bl}}{d\tau} = -k_e\beta^{bl}(\tau) + k_e\left(\hat{b} - \overline{u}_s\right) \quad (22)$$

To prove the ISPS stability of (22), as indicated in [7], an ISPS Lyapunov function should be found. Choosing $V = \frac{1}{2}\left(\beta^{bl}\right)^2$ as a candidate Lyapunov function, its time derivative would be as

$$\dot{V} = -k_e\left(\beta^{bl}(\tau)\right)^2 + k_e\beta^{bl}(\tau)\left(\hat{b} - \overline{u}_s\right) \quad (23)$$

which yields the inequality,

$$\dot{V} \leq -k_e\left(\beta^{bl}(\tau)\right)^2 + k_e\left|\beta^{bl}(\tau)\right|\left|\hat{b}\right| + k_e\left|\beta^{bl}(\tau)\right||\overline{u}_s| \quad (24)$$

adding and subtracting $k_e c\left(\beta^{bl}(\tau)\right)^2$ where $c \in (0, 1)$, and then by collecting the common terms it can be written:

$$\dot{V} \leq -2k_e(1 - c)V$$
$$- ck_e\left|\beta^{bl}(\tau)\right|\left(\left|\beta^{bl}(\tau)\right| - \frac{1}{c}\left|\hat{b}\right| - \frac{1}{c}|\overline{u}_s|\right) \quad (25)$$

and finally

$$\dot{V} \leq -2k_e(1 - c)V \quad if \quad \left|\beta^{bl}(\tau)\right| > \frac{1}{c}\left|\hat{b}\right| + \frac{1}{c}|\overline{u}_s| \quad (26)$$

or equivalently

$$\dot{V} \leq -2k_e(1 - c)V \quad if \quad V > max\left\{\frac{\left|\hat{b}\right|^2}{c^2}, \frac{|\overline{u}_s|^2}{c^2}\right\} \quad (27)$$

which proves that the selected Lyapunov function is ISPS. In terms of trajectory, for $\beta^{bl}(0) > 0$, there exists positive constants $l > 0$ and $d > 0$ such that the following equation holds [15]:

$$\left\|\beta^{bl}(\tau)\right\| \leq l\left\|\beta^{bl}(0)\right\|e^{-k_e\tau} + d \quad (28)$$

It should be noted that, d in (28) is proportional to the integral of the second term in (28). In the average, when the input gets close enough to the optimal input (u^*), if the assumption 3 does not hold it leads to $u^* + a\sin(\tau)$ crosses one of the limits so the system frequently switches between cases 1 and 2, then the value of d keeps increasing. The assumption 3 is

needed to avoid these switching in the steady state case and ensure that the system in steady state is working in case 1.

To prove the stability for other types of penalty function, one can notice that the f_{AW} in (20) is always having the following form:

$$f_{AW} = (u - D(u)) \mathbf{E}(u - D(u)) \tag{29}$$

where $\mathbf{E}(u - D(u))$ is a positive even function. Therefore

$$\omega \frac{d\beta^{bl}}{d\tau} = -k_e (u - D(u)) \mathbf{E}(u - D(u)) \tag{30}$$

Furthermore, by assuming $V_{new} = V = \frac{1}{2}\left(\beta^{bl}\right)^2$ we have:

$$\dot{V}_{new} = \frac{\partial V_{new}}{\partial \beta^{bl}} \frac{\beta^{bl}}{\partial \tau} = -k_e \frac{\partial V_{new}}{\partial \beta^{bl}} \mathbf{E}(u - D(u))(u - D(u))$$

or equivalently

$$\dot{V}_{new} = \dot{V} \ \mathbf{E}(u - D(u)) \tag{31}$$

therefore, according to inequality (27), we have

$$\dot{V}_{new} \le -2k_e(1-c)\mathbf{E}(u - D(u))V \tag{32}$$

which means that the new Lyapunov function candidate has the necessary conditions for ISPS stability (as $\mathbf{E}(u - D(u))$ does not change the sign of right side) □

Remark 1. *Using the above lemma, it can be concluded that there exists an invariant set $M = \{\beta^{bl} \in \mathbb{R} : \|\beta^{bl}\| < r\}$ such that for all $\beta_0 \in M$, the trajectories of boundary layer systems (18) are confined to set M at the transient time t_l. We define the steady-state constant $\beta_{ss}^{bl} \in M$ such that $\lim_{t \to t_l} \beta^{bl}(t) = \beta_{ss}^{bl}$.*

After the convergence of the boundary layer subsystem, the slow manifold would be as

$$0 = f_{AW}(u, \boldsymbol{u_s}) \tag{33}$$

According to the property of the penalty function, when $u \in \boldsymbol{u_s}$, the equation (33) becomes zero, which yields the steady-state $\beta^{bl} + D(u) = \hat{u} + a\sin(\omega t)$. The equilibrium of interest is $\hat{u}^* = u^* + \beta_{ss}^{bl}$. Let $\tilde{u}(t) = \hat{u}(t) - \hat{u}^*$ and the error of Hessian estimate be $\tilde{\gamma} = \gamma - H^{-1}$, where H is equivalent to $h(.)^{(n+2)}$, the corresponding error dynamics associated with the reduced system are given by:

$$\frac{d\tilde{u}^r}{d\tau} = -\epsilon \hat{k}_I(\tilde{\gamma}^r + H^{-1})\Upsilon_{n+1}h(\tilde{u}^r + u^* + a\sin(\tau)) \tag{34a}$$

$$\frac{d\tilde{\gamma}^r}{d\tau} = \epsilon \hat{k}_R(\tilde{\gamma}^r + H^{-1})\Big(1 - (\tilde{\gamma}^r + H^{-1})\Upsilon_{n+2}$$
$$\times h(\tilde{u}^r + u^* + a\sin(\tau))\Big) \tag{34b}$$

The following lemma addresses the convergence properties of the reduced system.

Lemma 2. *Consider the reduced system (34) under the Assumptions 1 and 2. There exists an $\bar{a} > 0$ and for any $a \in (0, \bar{a})$, there exists an $\bar{\epsilon} > 0$ such that for all $\epsilon \in (0, \bar{\epsilon})$, the solution of system (34) exponentially converges to the neighborhood of the origin with an error of order $O(\epsilon + a^3)$.*

Proof. With ϵ assumed to be small enough, one can employ to the standard averaging theory [14] on (34). In addition, we utilize the Taylor series of $h(\tilde{u}^r + u^* + a\sin(\omega t))$ of the following form:

$$h_\infty(.) = \sum_{i=0}^\infty \frac{a^i}{i!} h^{(i)}(\tilde{u}^r + u^*) \sin^i(\omega t) \tag{35}$$

As part of the averaging method, $\tilde{u}^r$ and $\tilde{\gamma}^r$ are frozen and replaced with autonomous values $\tilde{u}_{av}^r$ and $\tilde{\gamma}_{av}^r$. So using (35), the average of the reduced-order system (34) is:

$$\frac{d\tilde{u}_{av}^r}{d\tau} = -\epsilon \hat{k}_I(\tilde{\gamma}_{av}^r + H^{-1})\eta_{n+1}(\tilde{u}_{av}^r + u^*) \tag{36a}$$

$$\frac{d\tilde{\gamma}_{av}^r}{d\tau} = \epsilon \hat{k}_R(\tilde{\gamma}_{av}^r + H^{-1})\Big(1 - (\tilde{\gamma}_{av}^r + H^{-1})\eta_{n+2}(\tilde{u}_{av}^r + u^*)\Big) \tag{36b}$$

where

$$\eta_j(\tilde{u}_{av}^r + u^*) = AVE\left\{\Upsilon_j h(\tilde{u}_{av}^r + u^* + a\sin(\tau))\right\}$$
$$= h^{(j)}(\tilde{u}_{av}^r + u^*) + \frac{h^{(j+2)}(\tilde{u}_{av}^r + u^*)}{4(j+1)}a^2 + O(a^4) \tag{37}$$

In which AVE is an averaging operator that fulfills the well-defined average property given in Definition 3. This formula is explained in detail in [8].

The right sides of (36) are set to zero to determine the equilibrium conditions. When $\hat{k}_R > 0$, it is clear that the differential Riccati equation has an unstable equilibrium at origin. So if the initial condition, $\gamma(0)$, is chosen such that $sign(\gamma(0)) = sign(h^{(n+2)}(u^*))$, it guarantees the inequality $(\tilde{\gamma}_{av}^r + H^{-1}) \ne 0$. Therefore the system of average errors must meet the following conditions to reach the equilibrium.

$$\eta_{n+1}(\tilde{u}_{av}^r + u^*) = 0 \tag{38a}$$

$$(\tilde{\gamma}_{av}^r + H^{-1})\eta_{n+2}(\tilde{u}_{av}^r + u^*) = 1 \tag{38b}$$

The solutions of (38) were already stated in [8] as

$$\tilde{u}_{avE} = \tilde{u}^* + O(a^3) \tag{39a}$$

$$\tilde{\gamma}_{avE} = \tilde{\gamma}^* + O(a^3) \tag{39b}$$

where

$$\tilde{u}^* = \frac{h^{(n+3)}(0)}{4(n+1)h^{(n+2)}(0)}a^2 \tag{40a}$$

$$\tilde{\gamma}^* = \frac{(h^{(n+3)}(0))^2}{4(n+1)(h^{(n+2)}(0))^3}a^2 + \frac{(h^{(n+4)}(0))^2}{4(n+3)(h^{(n+2)}(0))^2}a^2 \tag{40b}$$

Alternatively, there is a quadratic function that approximates all maps satisfying Assumption 1.

$$h^{(n)}(D(u)) = h^* + \frac{H}{2}(D(u) - u^*)^2 \tag{41}$$

Since $h^{(n+3)}(0) = h^{(n+4)}(0) = 0$ in phrase (40), the equilibrium point (39) is $(\tilde{u}_{avE}, \tilde{\gamma}_{avE}) = (0, 0)$, and the Jacobian of the system (36) evaluated at this equilibrium point is

$$\boldsymbol{A} = \begin{bmatrix} -\hat{k}_I & 0 \\ 0 & -\hat{k}_R \end{bmatrix} \tag{42}$$

Since A is Hurwitz the exponential stability of system (36) is guaranteed and according to [14, Theorem 8.4], the the reduced system (34) is exponentially stable. $\square$

To finalize the overall stability of the closed-loop system containing the slow and fast subsystems, the *closeness of solution* method, presented in [17], will be used. This method is a modified version of classical singular perturbation method in which unlike the classical method that needs the convergence of slow subsystem to a point, only convergence to a bounded set is needed.

A. Closeness of Solutions

Following the approach proposed in [17], let the time horizon $[0, T]$, be separated in sub-intervals $[t_l, t_{l+1}]$. The sub-intervals have the same length ϵS_ϵ, where S_ϵ is a function of time such that $\lim_{\epsilon \to 0} S_\epsilon = +\infty$.

We reformulate the system (13) in the following compact form:

$$\frac{dz}{d\tau} = g(x, z, \epsilon) \qquad (43)$$

$$\frac{dx}{d\tau} = \epsilon f(x, z, \epsilon) \qquad (44)$$

where $x = (\hat{u}, \gamma)$ and $z = \beta$. $x_{av}^r = (\tilde{u}_{av}^r, \tilde{\gamma}_{av}^r)$ denotes to the average of the reduced system.

Before presenting the main theory, the following notations, assumptions, and definitions are introduced.

Denote the trajectories of the boundary layer system (18) by $\phi^b(\tau, x, \beta_0)$, all starting at the forward invariant set $\beta_0 \in M$, as mentioned in Remark 1.

Assumption 4. $f(x, \phi^b, \epsilon)$ has a well-defined average $f_{av}(x)$ with the convergence function $\sigma(T)$.

Definition 3. *Denote the solution of system (13) for $t \in [0, T]$ by $(x(t), z(t))$ and $x(0) \in B_R(0)$. Define $\xi(t)$ for $t \in [t_l, t_{l+1}]$ as*

$$\xi(t) = \xi_l + \int_{t_l}^t f(\xi_l, y(s), 0) ds \qquad (45)$$

where $\xi(t_l) = \xi_l$ and $\xi_0 = x_0$, where $y(t)$ is the unique solution to

$$\frac{d\varsigma}{d\tau} = g(\xi_l, \varsigma(t), 0), \quad y(t_l) = z(t_l) \qquad (46)$$

Assumption 5. *The initial set $x(0) \in B_R(0)$ is invariant with respect to $\xi(t)$.*

Remark 2. *Since f and g are sufficiently smooth functions, they satisfy locally Lipschitz condition, with the Lipschitz constant $L > 0$. Therefore there exists an upper limit P on f and g, i.e.:*

$$\exists P, \quad P > 0 : \quad \|f(x, z, \epsilon)\| \le P, \quad \|g(x, z, \epsilon)\| \le P \quad (47)$$

We define

$$\Delta_l(t) := \max_{t_l \le s \le t} \|x(s) - \xi(s)\| \qquad (48)$$

$$d_l(t) := \max_{t_l \le s \le t} \|x(s) - \xi_l\| \qquad (49)$$

$$D_l(t) := \max_{t_l \le s \le t} \|z(s) - \varsigma(s)\| \qquad (50)$$

Assumption 6. *The reduced average system f_{av} is globally Lipschitz with Lipschitz constant $L_{av} > 0$.*

Lemma 3. *Consider the map $\epsilon \to S_\epsilon$ and suppose a compact set $B_R(0) \times M$ on which Assumption 4 holds. Then for any finite $T > 0$ and for $t \in [0, T]$, the upper bound of $\Delta_l(t)$ and $D_l(t)$ are given as*

$$\bar{\Delta}(\epsilon) := \big(2\epsilon S_\epsilon P + TL(\epsilon S_\epsilon P + \epsilon)(1 + LS_\epsilon e^{LS_\epsilon})\big)$$
$$e^{TL(1+S_\epsilon L e^{LS_\epsilon})} \qquad (51)$$

$$\bar{D}(\epsilon) := LS_\epsilon(\bar{\Delta}(\epsilon) + \epsilon S_\epsilon P + \epsilon)e^{LS_\epsilon} \qquad (52)$$

Proof. The proof of this lemma follows the same path as proof of [17, Lemma2]. $\square$

Theorem 1. *Suppose that there exist $R > 0$, ϵ_1 and compact set M such that Assumptions 1-5 hold on $(x, z, \epsilon) \in B_R(0) \times M \times (0, \epsilon_1]$. Then for any finite time interval $t \in [0, T]$, the trajectories of the perturbed slow dynamics $x(t)$ and the average of the reduced order of system $x_{av}^r(t)$ satisfies*

$$\|x(t) - x_{av}^r(t)\| \le K(\epsilon) \qquad (53)$$

where

$$K(\epsilon) := \bar{\Delta}(\epsilon) + T\sigma(S_\epsilon) + \epsilon S_\epsilon L_{av}\left(\epsilon S_\epsilon P + T\sigma(S_\epsilon)\right)e^{\epsilon S_\epsilon L_{av}}$$

Proof. The obtained results presented in lemma 1 and lemma 2 together with the assumptions 1-6 suffice to prove the stability according to [17, Theorem 1]. $\square$

Remark 3. *By virtue of uniformly exponential equilibrium point of system (36) in lemma 2, there exist positive constants r_x and B_x such that $\|x_{av}^r(t)\| = r_x e^{-B_x t}\|x_0\|$.*

Therefore the upper bound $\|x(t)\|$ is given by

$$\|x(\tau)\| \le r_x e^{-B_x t}\|x_0\| + K(\epsilon) \qquad (54)$$

IV. SIMULATION RESULTS

In order to evaluate the offered ES scheme for constrained input, we consider the following static map

$$y = 2D_{sat}(u) - (D_{sat}(u) - 0.5)^3 \qquad (55)$$

where the lower and upper bounds of actuator are $u_{min} = -1.4$ and $u_{max} = 2$, respectively. Simulation results for the system without and with anti-windup (using two different penalty functions) are shown in Fig. 2. The penalty functions are

$$Q_b^{log}(.) = -ln((u - D(u))^2 + 0.01) \qquad (56)$$

$$Q_b^p(.) = -(u - D(u))^2 \qquad (57)$$

with the corresponding anti-windup function

$$f_{AW1} = \frac{-2(u - D(u))}{(u - D(u))^2 + 0.01} \qquad (58)$$

$$f_{AW2} = -2(u - D(u)) \qquad (59)$$

The parameters for simulation were chosen as: $\omega = 60, a = 0.3, \epsilon = \frac{1}{3500}, \hat{k}_I = \hat{k}_R = 10$ and $k_e = 5$, and initial conditions $\hat{u} = -3, \gamma(0) = -0.01$ and $\beta(0) = 0$.
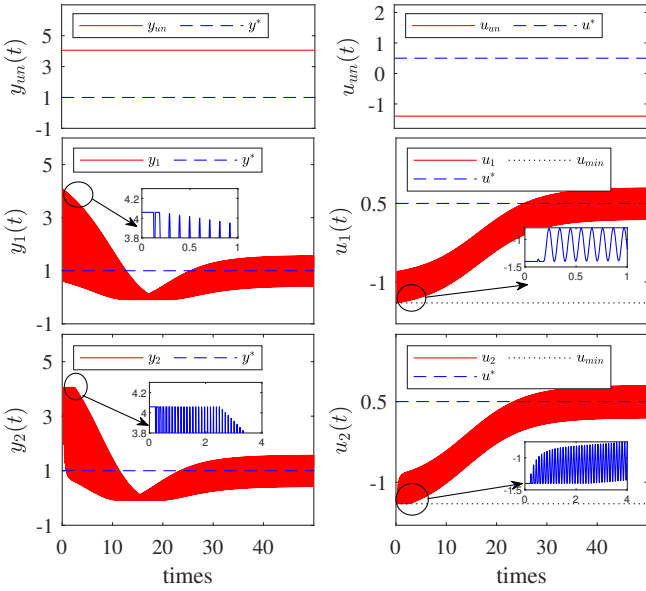
Fig. 2: Minimization of first derivative of the map upon saturated input. The output and input without anti-windup are given in a couple of top plots and the results with anti-windup are shown in the two couple of bottom plots.
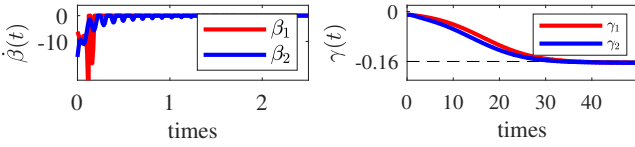

Fig. 3: Evaluation of $\dot{\beta}$ and γ for different types of f_{AW}.

Fig.2 shows the output of the system in different situations. As expected, without an anti-windup loop, the system's output gets stuck at an improper value. Moreover, it should be noted that when y is constant, $\dot{\gamma}$ is constant as well which means that $\|\gamma\|$ keeps increasing and makes the loop unstable. In Fig.2, four bottom plot demonstrate that, despite entering the saturation area, the system converges to the desired steady-state when the anti-windup loop is activated. The difference in the type of f_{AW} only affects the transient behavior.

The left plot of Fig.3 illustrates the function of the anti-windup loop, while the right plot shows that the Riccati equation has been able to estimate the inverse of Hessian appropriately ($H^{-1} = \frac{-1}{6}$).

V. CONCLUSION

This paper proposes an anti-windup mechanism for higher derivative Newton-based ES to address the scenarios where the input range is constrained. To analyze the stability of the proposed method a two-time-scaled decomposition of the system dynamics is utilized. A fast dynamic is considered for the anti-windup mechanism, while a slow dynamic is considered for the rest. To assess the overall stability of the closed-loop system, the closeness of the solution method was used. Finally, we used a classical example, using a static map, to illustrate the effectiveness of the proposed method compared with the case where no anti-windup mechanism was used.

REFERENCES

[1] M. Leblanc, "Sur l'electrification des chemins de fer au moyen de courants alternatifs de frequence elevee," *Revue générale de l'électricité*, vol. 12, no. 8, pp. 275–277, 1922.

[2] M. Krstic and H.-H. Wang, "Stability of extremum seeking feedback for general nonlinear dynamic systems," p. 7, 2000.

[3] Y. Tan, W. H. Moase, C. Manzie, D. Nešić, and I. M. Y. Mareels, "Extremum seeking from 1922 to 2010," in *Proceedings of the 29th Chinese Control Conference*. IEEE, 2010, pp. 14–26.

[4] J. I. Poveda and M. Krstic, "Fixed-time extremum seeking," *arXiv preprint arXiv:1912.06999*, 2019.

[5] M. Ghadiri-Modarres and M. Mojiri, "Normalized extremum seeking and its application to nonholonomic source localization," *IEEE Transactions on Automatic Control*, vol. 66, no. 5, pp. 2281–2288, 2020.

[6] S.-J. Liu and M. Krstic, "Newton-based stochastic extremum seeking," *Automatica*, vol. 50, no. 3, pp. 952–961, 2014.

[7] A. Ghaffari, M. Krstić, and D. Nešić, "Multivariable Newton-based extremum seeking," *Automatica*, vol. 48, no. 8, pp. 1759–1767, Aug. 2012.

[8] G. Mills and M. Krstic, "Maximizing map sensitivity and higher derivatives via extremum seeking," *IEEE Transactions on Automatic Control*, vol. 63, no. 10, pp. 3232–3247, 2018.

[9] K. Vinther, H. Rasmussen, R. Izadi-Zamanabadi, and J. Stoustrup, "Single temperature sensor superheat control using a novel maximum slope-seeking method," *international journal of refrigeration*, vol. 36, no. 3, pp. 1118–1129, 2013.

[10] D. Rušiti, T. R. Oliveira, M. Krstić, and M. Gerdts, "Newton-based extremum seeking of higher-derivative maps with time-varying delays," *International Journal of Adaptive Control and Signal Processing*, vol. 35, no. 7, pp. 1202–1216, 2021.

[11] G. Shao, A. R. Teel, Y. Tan, K.-Z. Liu, and R. Wang, "Extremum seeking control with input dead-zone," *IEEE Transactions on Automatic Control*, vol. 65, no. 7, pp. 3184–3190, 2019.

[12] Y. Tan, Y. Li, and I. M. Mareels, "Extremum seeking for constrained inputs," *IEEE Transactions on Automatic Control*, vol. 58, no. 9, pp. 2405–2410, 2013.

[13] M. Guay, "Mixed-integer extremum seeking control for unknown static maps," in *2020 European Control Conference (ECC)*. IEEE, 2020, pp. 1256–1261.

[14] H. K. Khalil, *Nonlinear systems; 3rd ed.* Prentice-Hall, 2002.

[15] Z.-P. Jiang, I. M. Mareels, and Y. Wang, "A lyapunov formulation of the nonlinear small-gain theorem for interconnected iss systems," *Automatica*, vol. 32, no. 8, pp. 1211–1215, 1996.

[16] W. H. Moase, C. Manzie, and M. J. Brear, "Newton-Like Extremum-Seeking for the Control of Thermoacoustic Instability," *IEEE Transactions on Automatic Control*, vol. 55, no. 9, pp. 2094–2105, Sep. 2010.

[17] M. Deghat, S. Ahmadizadeh, D. Nešić, and C. Manzie, "Closeness of solutions for singularly perturbed systems via averaging," in *2018 IEEE Conference on Decision and Control (CDC)*. IEEE, 2018, pp. 3110–3115.